IEEE Access
Multidisciplinary | Rapid Review | Open Access Journal

Received February 27, 2019, accepted March 11, 2019, date of publication March 14, 2019, date of current version April 8, 2019.

Digital Object Identifier 10.1109/ACCESS.2019.2904943

Adaptive Virtual Inertia Control Strategy of VSG for Micro-Grid Based on Improved Bang-Bang Control Strategy

JIN LI, BUYING WEN, AND HUAIYUAN WANG

Fujian Smart Electrical Engineering Technology Research Center, College of Electrical Engineering and Automation, Fuzhou University, Fuzhou 350116, China

Corresponding author: Huaiyuan Wang (79749544@qq.com)

ABSTRACT With the increasing capacity of new energy in the power system, new energy cannot provide support for the system frequency directly. This characteristic of new energy affects the frequency stability of the power system. Therefore the control strategy of a virtual synchronous generator (VSG) is proposed to improve the frequency stability of the system. An adaptive virtual inertia control strategy based on an improved bang-bang control strategy for a micro-grid is presented. On one hand, it can make full use of the variability of virtual inertia to reduce dynamic frequency deviation. On the other hand, the steady-state interval of frequency and the steady-state inertia are set to improve the system frequency stability. Then the stability analysis of the value range of the virtual inertia is performed by the small signal model of the VSG for the micro-grid. Meanwhile, the ranges of virtual inertia and steady-state inertia are determined. Finally, Matlab/Simulink is applied to accomplish simulation experiments to compare various virtual inertia control strategies. The results indicate the effectiveness of the proposed strategy.

INDEX TERMS Adaptive virtual inertia, bang-bang control strategy, micro-grid, virtual synchronous generator.

I. INTRODUCTION

With the exhaustion of traditional fossil energy, the reform of energy structure has become the focus of social concern. Most renewable energy is connected to a power grid by grid-connected inverters [1]. However, due to the existence of grid-connected inverter, the new energy cannot provide inertia support for the power system as the traditional synchronous generator, which makes the power parameters respond too quickly when the system is disturbed. Contemporarily, renewable energy accounts for a larger and larger proportion of power system capacity. And its influence on the stability of the power system cannot be ignored. Therefore, renewable energy needs to have certain frequency support capacity to maintain the stable operation of a power grid [2].

To achieve frequency regulation, the droop control strategy is put forward [3]–[7]. The function of primary frequency regulation is realized by the droop control strategy. Then, the output power of the inverter can be adjusted according to the fluctuation of the power grid frequency. Thus frequency regulation capacity is provided by new energy for the power grid. However, the ability to provide inertia support for the power grid is not contained by the droop control strategy. Therefore, when the active load is suddenly changed, the frequency of the power grid will shake rapidly because of the lack of inertia.

In order to provide inertial support, the concept of the virtual synchronous generator (VSG) is advocated in the literature [8]–[14]. The external characteristics of the synchronous generator are simulated by VSG. On the basis of realizing the function of primary frequency regulation, the inertial support is also realized. The frequency stability of the power grid is improved by the virtual inertia.

As the core part of VSG, many scholars have conducted relevant research on virtual inertia. The flexible VSG control strategy with adaptive inertia is recommended in [15]. When the frequency change rate is greater than the threshold, its inertia increases with the rate of frequency change. But the specific selection method of coefficients is not mentioned. A fuzzy controller is applied to determine the virtual inertia [16]. The fuzzy rule is that the virtual inertia changes with the angular velocity and angular velocity deviation. Although fuzzy rules are given, the method of setting the numerical value of inertia is not presented. A VSG control strategy

The associate editor coordinating the review of this manuscript and approving it for publication was Feng Liu.

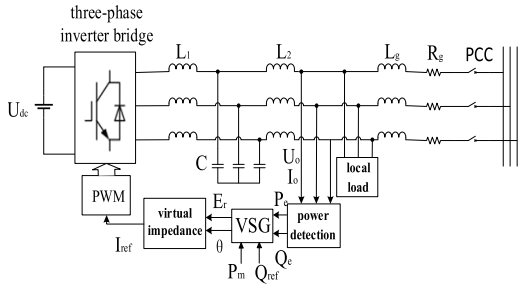

FIGURE 1. Topology and control structure of the VSG.

based on bang-bang control strategy is introduced in [17]. The virtual inertia is adjusted with the change of frequency to the maximum or minimum value. However, no setting method of maximum and minimum of the virtual inertia is given. An adaptive virtual inertia control strategy is proposed in [18]. And the influence of virtual inertia size on system frequency is analyzed. But the specific method of setting virtual inertia and other related parameters are not introduced.

An adaptive virtual inertia control strategy of VSG for micro grid based on improved bang-bang control strategy is presented in this paper. In order to improve frequency stability in the steady state, a steady-state frequency interval and inertia are set. When the frequency exceeds the steady-state interval, the virtual inertia is adaptively changed to the maximum or minimum value based on the frequency change rate and deviation. By small signal model of the VSG for the micro-grid, the stability of the virtual inertia is analyzed and the range of the virtual inertia is determined. Finally, Matlab/Simulink is applied to verify the effectiveness of the proposed strategy.

II. THE FUNDAMENTALS OF VSG

The main circuit topology and control structure of VSG are shown in figure 1 [19]. It mainly consists of the following parts: direct current (DC) power supply, three-phase inverter bridge, LCL filter, line impedance, local load, the point of common coupling (PCC), and control loop. Where, the control loop includes the power detection module, the VSG module, the virtual impedance [20] module, and the PWM module.

The rotor motion equation of a synchronous generator whose number of poles is 1 is simulated by the active power loop of VSG, as shown in (1):

$$\begin{cases} J\dfrac{d\omega}{dt} = \dfrac{P_m}{\omega_N} - \dfrac{P_e}{\omega_N} - D_{\mathrm{p}}(\omega - \omega_N) \\ \dfrac{d\theta}{dt} = \omega \end{cases} \tag{1}$$

where J is rotational inertia, ω is rotor angular velocity; P_m and P_e are mechanical power and electromagnetic power, respectively; ω_N is rotor rated angular velocity; D_p is the damping coefficient, and θ is the power angle.

An integrator is added to the damping link to realize the function of secondary frequency regulation. The control

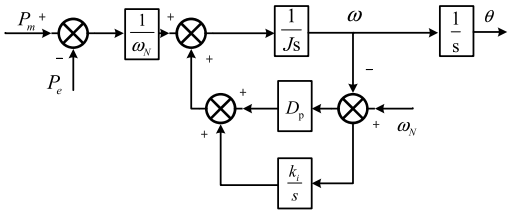

FIGURE 2. The active-power loop of the VSG with the function of secondary frequency regulation.

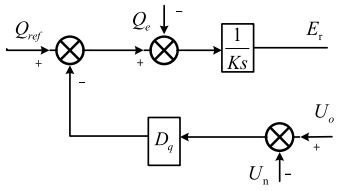

FIGURE 3. The reactive-power loop of the VSG.

block diagram, in which k_i is the integral gain, is indicated in figure 2.

The active power loop is simulated by the reactive power loop to realize the voltage regulation function, as manifested in (2):

$$K\frac{dE_r}{dt} = Q_{\mathrm{ref}} - Q_{\mathrm{e}} - D_{\mathrm{q}}(U_{\mathrm{o}} - U_n) \tag{2}$$

where K is the reactive power-voltage inertia coefficient of the reactive power loop, E_r is the virtual electromotive force, Q_{ref} is the reference reactive power, Q_e is the reactive power output; D_q is the reactive power-voltage droop coefficient; U_o is the output voltage amplitude, and U_n is the rated voltage amplitude.

III. ADAPTIVE VIRTUAL INERTIA CONTROL STRATEGY

Formula (1) can be translated into the following form, as revealed in (3):

$$J\frac{d\omega}{dt} = \frac{\Delta P}{\omega_N} - D_{\mathrm{p}}\Delta\omega \tag{3}$$

where ΔP is the active power deviation, and $\Delta\omega$ is rotor angular velocity deviation.

In the interval t_0-t_1, the load decreases at t_0, and the ΔP increases suddenly. According to equation (3) and figure 4, $\Delta\omega$ keeps constant at t_0 which results in J(dω/dt) increasing sharply. Because J is a fixed value, dω/dt increases suddenly. Then dω/dt fell to 0 at t_1. At the same time, $\Delta\omega$ is increased to maximum. In the interval t_0-t_1, we can appropriately increase J to limit the value of dω/dt, reducing the maximum $\Delta\omega$.

In the interval t_1-t_2, $\Delta\omega$ recurs to 0 at t_2. And dω/dt slowly backs to 0 after be decreased to the minimum. In the interval t_1-t_2, we can appropriate reduce J to reduce the value of dω/dt so that making $\Delta\omega$ return to 0 more quickly.

The situations in the interval t_2-t_3 and interval t_3-t_4 are similar to those in interval t_0-t_1 and interval t_1-t_2. The virtual inertia should be appropriately adjusted to make frequency response characteristics better. The adjustment of inertia is listed in Table 1.

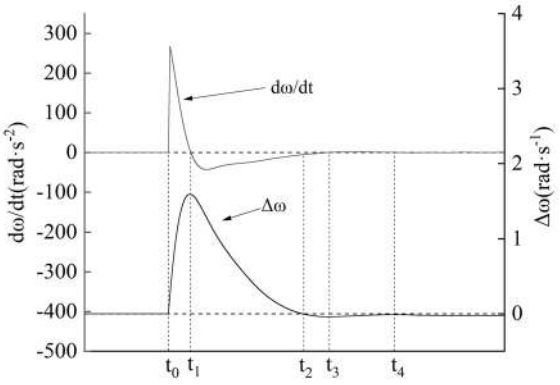

FIGURE 4. The relationship between dω/dt and Δω of load shedding.

TABLE 1. The adjustment of virtual rotor inertia.

Interval	Δω	dω/dt	Δω(dω/dt)	Adjustment of inertia
t_0-t_1	>0	>0	>0	Increase
t_1-t_2	>0	<0	<0	Decrease
t_2-t_3	<0	<0	>0	Increase
t_3-t_4	<0	>0	<0	Decrease

When $\Delta\omega$ and dω/dt have the same sign, the virtual inertia should be enhanced. When $\Delta\omega$ and dω/dt have different signs, the virtual inertia should be weakened.

For the traditional adaptive virtual inertia strategy based on bang-bang control strategy, the virtual inertia is regulated to the maximum or minimum adaptively with the rate of change of frequency and deviation of frequency. An adaptive virtual inertia strategy based on improved bang-bang control strategy is proposed in this paper.

A steady-state frequency interval is set to avoid the frequency fluctuation in steady state. Small disturbance of frequency may lead to the fluctuation of inertia. However, the fluctuation of inertia will impact the stability of frequency indirectly. When the frequency exceeds the steady-state interval, the virtual inertia is adaptively changed to the maximum or minimum with the product of the change rate and deviation of frequency. The steady-state inertia selected between the maximum and the minimum of the virtual inertia is set for the steady-state interval.When the frequency is in the steady-state interval, the virtual inertia keeps steady-state inertia. Then the frequency will not response moderative because of the maximum of the virtual inertia. Meanwhile, the frequency won't have a large deviation because of being disturbed with the minimum inertia. Thus, the improved bang-bang control strategy is proposed as rendered in (4).

$$J = \begin{cases} J_{\max}, & \Delta\omega \dfrac{d\omega}{dt} > 0 \cap |\Delta\omega| > 2\pi f_s \\ J_{\min}, & \Delta\omega \dfrac{d\omega}{dt} \le 0 \cap |\Delta\omega| > 2\pi f_s \\ J_s, & |\Delta\omega| \le 2\pi f_s \end{cases} \tag{4}$$

where J_{max}, J_{min}, and J_s are the maximum value, the minimum value, and the fixed values at steady state of the virtual inertia, respectively; f_s is the frequency deviation of the steady-state interval.

The range of the virtual inertia and the selection of the steady-state inertia will be obtained by the small signal model analysis in the following chapters.

IV. THE SMALL SIGNAL MODEL

The equivalent circuit of VSG for micro-grid is displayed in figure 5.

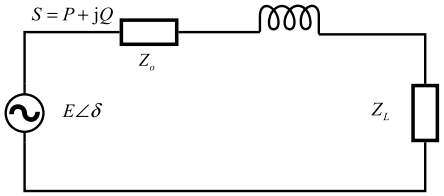

FIGURE 5. The equivalent circuit of inverter under micro-grid mode.

In figure 5, $E\angle\delta$ is the output voltage of the inverter; Z_o is the output impedance of the inverter; Z_L is the load impedance; the output power of the inverter is $S = P+jQ$, and the sum of the output impedance and the load impedance is $R+jX$, then

$$\begin{cases} P = \dfrac{RE^2(\cos^2\delta - \sin^2\delta) + 2XE^2\sin\delta\cos\delta}{R^2+X^2} \\ Q = \dfrac{2RE^2\sin\delta\cos\delta - XE^2(\cos^2\delta - \sin^2\delta)}{R^2+X^2} \end{cases} \tag{5}$$

The static working point is set as (E_S, δ_S). Then the relationship among power angle disturbance $\Delta\delta$, voltage disturbance ΔE and active power disturbance ΔP, reactive power disturbance ΔQ is got, as shown in (6).

$$\begin{cases} \Delta P = K_{pf}\Delta\delta + K_{pe}\Delta E \\ \Delta Q = K_{qf}\Delta\delta + K_{qe}\Delta E \end{cases} \tag{6}$$

where

$$\begin{cases} K_{pf} = \dfrac{2XE_s^2\cos 2\delta_s - 2RE_s^2\sin 2\delta_s}{R^2+X^2} \\ K_{pe} = \dfrac{2RE_s\cos 2\delta_s + 2XE_s\sin 2\delta_s}{R^2+X^2} \\ K_{qf} = \dfrac{2RE_s^2\cos 2\delta_s + 2XE_s^2\sin 2\delta_s}{R^2+X^2} \\ K_{qe} = \dfrac{2RE_s\sin 2\delta_s - 2XE_s\cos 2\delta_s}{R^2+X^2} \end{cases}$$

For the purpose of simplifying the analysis, the active and reactive power loops are approximately decoupled with the control of virtual impedance in this paper. According to figure 2 and (2), (5) and (6), the small signal equivalent model of VSG for the micro-grid can be procured, as clarified in figure 6.

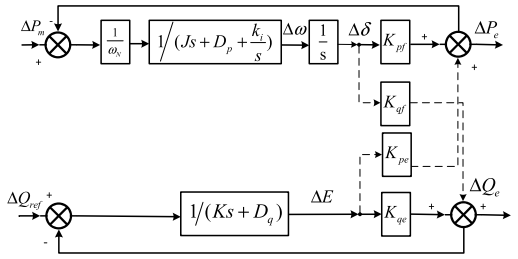

FIGURE 6. Small-signal equivalent model of VSG.

TABLE 2. Parameters settings for VSG algorithm.

Parameter	Value and quantity	Parameter	Value and quantity
U_{dc}	800V	C	10μF
U_{rms}	220V	L_2	800μH
S_N	10kW	E_s	226V
f_N	50Hz	δ_s	0.05
L_1	3.2mH	K_{pwm}	400
P_m	5kW	Q_{set}	2kvar
k_i	780	D_p	5Nm·s/rad

Then, the closed-loop transfer function of the active power loop is obtained, as shown in (7):

$$G_{\mathrm{p}} = \frac{K_{\mathrm{pf}}}{J\omega_N s^2 + D_{\mathrm{p}}\omega_N s + k_i\omega_N + K_{\mathrm{pf}}} \tag{7}$$

Some parameter settings of VSG control system can be set, as shown in Table 2.

According to (7), active power loop closed-loop transfer function of VSG is a typical second-order system.

The natural angular frequency is

$$\omega_{N\mathrm{p}} = \sqrt{(k_i + K_{\mathrm{pf}}/\omega_N)/J} \tag{8}$$

The damping ratio is

$$\xi = \frac{D_{\mathrm{p}}}{2\sqrt{J(k_i + K_{\mathrm{pf}}/\omega_N)}} \tag{9}$$

The amplification factor is

$$K_p = \frac{K_{\mathrm{pf}}/\omega_N}{k_i + K_{\mathrm{pf}}/\omega_N} \tag{10}$$

where the size of K_{pf} can be calculated from table 2 and (5). When the active and reactive power loops are approximately decoupled, K_{pf} is around 1.0×10^5.

The condition for the stability of the second order system is that the damping ratio $\xi > 0$. In order to make the VSG have a faster frequency response speed, the active power loop is made as an underdamping unit. Then $0< \xi <1$. Therefore, $J > 0$ can be calculated from $\xi > 0$. And $J > 0.0057$ can be obtained from $\xi < 1$.

According to the provisions of GB/T31464-2015 "grid operation standards", the unit's primary frequency regulation shall respond to frequency failure within 3s. Assuming that the response time of VSG participating in grid frequency regulation t_s is approximately equal to the response time of VSG active power loop t_p. Considering margin, t_p is set as t_p <1s.

The response time of a typical under-damping second-order link is shown in (11):

$$t_p = \frac{4.4}{\xi\omega_{Np}} \tag{11}$$

$J < 0.57$ can be obtained from $t_p = \dfrac{4.4}{\xi\omega_{Np}} < 1s$.

To sum up, the range of J is 0.0057<J<0.57.

The rotor inertia J of a synchronous generator is directly proportional to the inertial time constant H, as shown in (12).

$$H = J\omega_N^2 \Big/ S_N \tag{12}$$

where S_N is the rated power of the synchronous generator.

For a general synchronous generator, the value of the inertial time constant H ranges from 2s to 9s. Considering that the response time of VSG should not be too slow and the range of the rotor inertia obtained above, the steady-state virtual inertia is set as $J_s = 0.2028\mathrm{kg{\cdot}m^2}$.

V. SIMULATION RESULTS

For the purpose of verifying the correctness and superiority of the proposed control strategy, a system of VSG is built by MATLAB/Simulink software.

In the initial, the active load of 5kW and the reactive load of 2kvar are connected to the system. At 1s, the active load is increased to 10kW. At 1.5s, the load is returned to initial. With the same simulation conditions, three strategies are compared and verified.

For the strategy 0, the virtual inertia is set as a constant $J_s = 0.2028\mathrm{kg{\cdot}m^2}$. For the strategy I which proposed in this paper, the parameter is listed in Table 3. For the strategy II which proposed in [13], the main parameters are set as $J_0 = 0.2028\mathrm{kg{\cdot}m^2}$, $M_j = 5$, $k_j = 0.015$. For the strategy I, which proposed in [15], the main parameters are set as $J_0 = 0.2028\mathrm{kg{\cdot}m^2}$, $M = 5$, $k_1 = 0.015$, $k_2 = 2$. For the strategy II, the main parameters are set as $J_{max} = 0.57\ \mathrm{kg{\cdot}m^2}$, $J_{min} = 0.0057\ \mathrm{kg\cdot m^2}$.

TABLE 3. Simulation parameters.

Parameter	Value and quantity	Parameter	Value and quantity
J_s	$0.2028\mathrm{kg{\cdot}m^2}$	J_{min}	$0.0057\mathrm{kg{\cdot}m^2}$
J_{max}	$0.57\mathrm{kg{\cdot}m^2}$	f_s	0.004Hz

Control effect of different strategies is shown in figure 7. When the active load is suddenly increased at 1s, the frequency is decreased because of the loss of active power. Compared with the strategy 0, the strategy I, the strategy II, and the strategy III all have a smaller frequency deviation. Meanwhile, their control effects vary greatly in the frequency recovery process. Among them, the frequency of the strategy I can be restored to 50Hz as soon as possible; the recovery

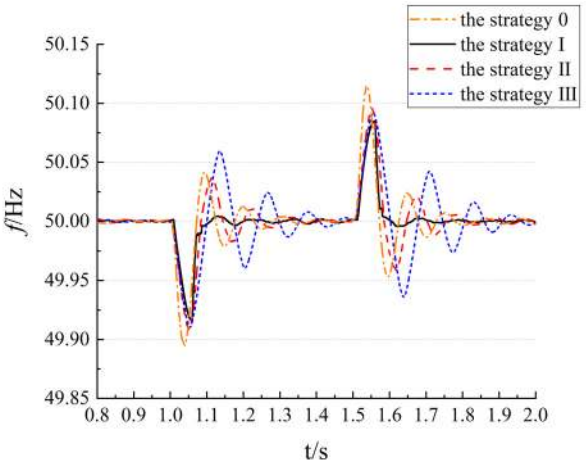

FIGURE 7. Control effect of different strategies.

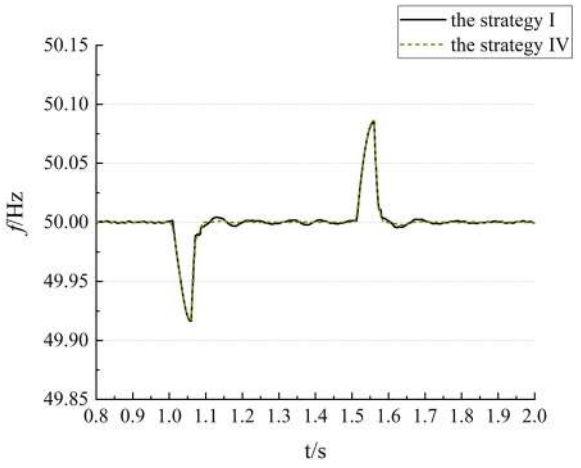

FIGURE 9. Control effect of the strategy I and the strategy IV.

process of strategy II is similar to that of the strategy 0; the control effect of the strategy III is the worst, the number of oscillation is the most and the overshoot is the largest in the process of frequency recovery. When the load returns to initial at 1.5s, the frequency is increased because of the residual of mechanical power. Similarly, when the load is dropped suddenly, the effects of the three control strategies are basically the same as the control effects when the load is increased suddenly.

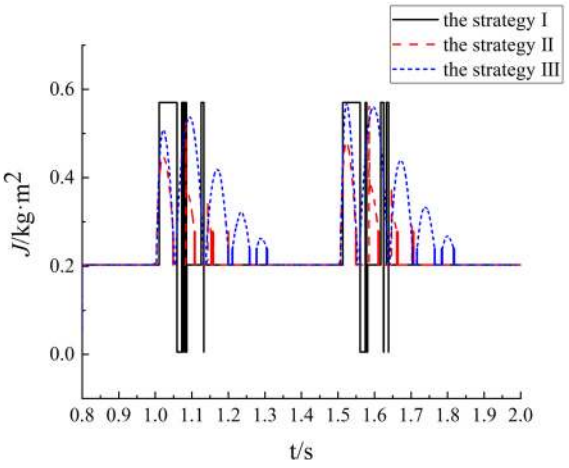

FIGURE 8. The curve of virtual inertia.

The curve of virtual inertia is shown in figure 8. For the strategy II and the strategy III, because of the limitation of the range of inertia, the constant k_j and k_1 cannot be oversized, which limits the adjustment of inertia in other cases.

For the strategy I, the virtual inertia is adjusted to the maximum when the frequency escapes the steady-state interval, then the frequency deviation is weakened. When the frequency returns to the steady state interval, the virtual inertia is decreased to the minimum, so that the recovery speed is accelerated.

It can be seen from figure 9 and figure 10 that the control effects of the strategy I and the strategy IV are basically the same, but the control of the virtual inertia is quite different. When the frequency is in the steady state interval, the virtual inertia of the strategy IV jumps frequently. However, for the strategy I, many redundant control actions are reduced.

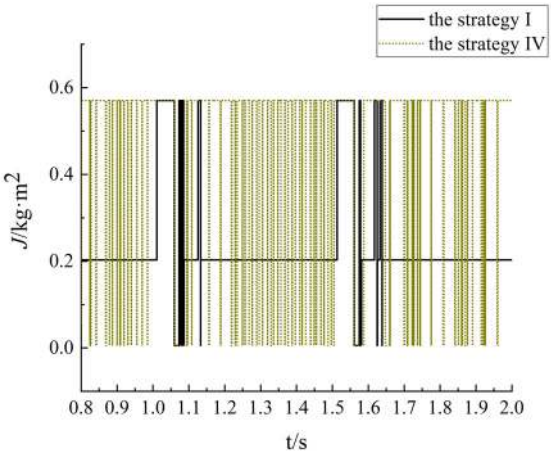

FIGURE 10. The curves of virtual inertia of the strategy I and the strategy IV.

VI. CONCLUSION

As can be seen from the simulation results, when the frequency is far away from the steady state interval, the increase of inertia can reduce the frequency deviation. Oppositely, when the frequency is close to the steady state interval, the reduction of inertia can make the recovery speed faster. What's more, the change of frequency does not cause the inertia to fluctuate frequently. Compared to the other strategies, the validity of the strategy present in this article is proved.

At present, only the relationship between active power and frequency is discussed in this paper, but the relationship between reactive power and voltage. In order to further improve the VSG power loop control scheme, the next step is to study the reactive power loop control strategy of the VSG.

REFERENCES

[1] F. Blaabjerg, R. Teodorescu, M. Liserre, and A. V. Timbus, "Overview of control and grid synchronization for distributed power generation systems," *IEEE Trans. Ind. Electron.*, vol. 53, no. 5, pp. 1398–1409, Oct. 2006.
[2] Y. V. P. Kumar and R. Bhimasingu, "Improving resiliency in renewable energy based green microgrids using virtual synchronous machines controlled inverter," in *Proc. IEEE Innov. Smart Grid Technol.-Asia (ISGT ASIA)*, Nov. 2015, pp. 1–6.
[3] U. B. Tayab, M. A. Roslan, L. J. Hwai, and M. Kashif, "A review of droop control techniques for microgrid," *Renewable Sustain. Energy Rev.*, vol. 76, pp. 717–727, Sep. 2017.
[4] J. W. Simpson-Porco, F. Dörfler, and F. Bullo, "Voltage stabilization in microgrids via quadratic droop control," *IEEE Trans. Autom. Control*, vol. 62, no. 3, pp. 1239–1253, Mar. 2017.
[5] U. B. Tayab, M. A. Roslan, L. J. Hwai, and M. A. Kashif, "A review of droop control techniques for microgrid,"*Renewable Sustain. Energy Rev.* vol. 76, pp. 717–727, Sep. 2017.
[6] X. Sun, Y. Hao, Q. Wu, X. Guo, and B. Wang, "A multifunctional and wireless droop control for distributed energy storage units in islanded AC microgrid applications," *IEEE Trans. Power Electron.*, vol. 32, no. 1, pp. 736–751, Jan. 2017.
[7] J. Schiffer, R. Ortega, A. Astolfi, J. Raisch, and T. Sezi, "Stability of synchronized motions of inverter-based microgrids under droop control," *IFAC Proc. Volumes*, vol. 47, no. 3, pp. 6361–6367, 2014.
[8] I. Serban and C. P. Ion, "Microgrid control based on a grid-forming inverter operating as virtual synchronous generator with enhanced dynamic response capability," *Int. J. Elect. Power Energy Syst.*, vol. 89, pp. 94–105, Jul. 2017.
[9] T. V. Van *et al.*, "Virtual synchronous generator: An element of future grids," in *Proc. IEEE PES Innov. Smart Grid Technol. Conf. Eur.*. Oct. 2010. pp. 1–7.
[10] Z. Lü, W. Sheng, and Q. Zhong, "Virtual synchronous generator and its applications in micro-grid," in *Proc. CSEE.*, vol. 34, Jun. 2014, pp. 2591–2603,
[11] J. Liu, Y. Miura, and T. Ise, "Comparison of dynamic characteristics between virtual synchronous generator and droop control in inverter-based distributed generators," *IEEE Trans. Power Electron.*, vol. 31, no. 5, pp. 3600–3611, May 2015.
[12] Q.-C. Zhong, P.-L. Nguyen, Z. Ma, and W. Sheng, "Self-synchronized synchronverters: Inverters without a dedicated synchronization unit," *IEEE Trans. Power Electron.*, vol. 29, no. 2, pp. 617–630, Feb. 2014.
[13] Y. Chen, R. Hesse, D. Turschner, and H. P. Beck, "Comparison of methods for implementing virtual synchronous machine on inverters," in *Proc. Int. Conf. Renew. Energies Power Qual.*, Mar. 2012, pp. 1–6.
[14] J. Alipoor, Y. Miura, and T. Ise, "Stability assessment and optimization methods for microgrid with multiple VSG units," *IEEE Trans. Smart Grid*, vol. 9, no. 2, pp. 1462–1471, Mar. 2018.
[15] J, Meng, Y. Wang, C. Fu, and H. Wang, "Adaptive virtual inertia control of distributed generator for dynamic frequency support in microgrid," in *Proc. IEEE Energy Convers. Congr. Expo.*, Sep. 2016, pp. 1–5.
[16] Y. Hu, W. Wei, Y. Peng, and J. Lei, "Fuzzy virtual inertia control for virtual synchronous generator," in *Proc. 35th Chin. Control Conf.*, Jul. 2016, pp. 8523–8527.
[17] J. Alipoor, Y. Miura, and T. Ise, "Power system stabilization using virtual synchronous generator with alternating moment of inertia," *IEEE Trans. Emerg. Sel. Topics Power Electron.*, vol. 3, no. 2, pp. 451–458, Jun. 2015.
[18] D. Li, Q. Zhu, S. Lin, and X. Y. Bian, "A self-adaptive inertia and damping combination control of VSG to support frequency stability," *IEEE Trans. Energy Convers.*, vol. 32, no. 1, pp. 397–398, Mar. 2017.
[19] W. Heng, R. Xinbo, Y. Dongsheng, C. Xinran, Z. Qingchang, and L. Zhipeng, "Modeling of the power loop and parameter design of virtual synchronous generators," in *Proc. (CSEE)*, Jun. 2015, pp. 6508–6518.
[20] P. Zhang, H. Zhao, H. Cai, J. Shi, and X. He, "virtual negative resistor for inverters low-voltage microgrids," *IET Power Electron.*, vol. 9, no. 5, pp. 1037–1044, 2016.

JIN LI received the B.Sc. degree in electrical engineering from Fuzhou University, China, in 2013, where he is currently pursuing the master's degree. His research interests include new energy and energy storage technologies, virtual synchronous generator, and inverter control.

BUYING WEN received the B.Eng., master's, and Ph.D. degrees from Fuzhou University, in 1991, 1998, and 2006, respectively, all in electrical engineering. He is currently a Professor with the College of Electrical Engineering and Automation, Fuzhou University. His research interests include power market and wind power operation technology.

HUAIYUAN WANG received the B.Eng. and Ph.D. degrees in electrical engineering from Xian Jiaotong University, in 2010 and 2016. He is currently with the College of Electrical Engineering and Automation, Fuzhou University. His research interests include power systems modeling, power systems protection, and power systems stability and control.